Journal of Biomechanical Science and Engineering

Vol. 6, No. 2, 2011

Residual Stress Distribution in the Bovine Femoral Diaphysis Measured by Synchrotron*

Satoshi YAMADA**, Shigeru TADANO***,
Masahiro TODOH*** and Kazuhiro FUJISAKI***
**Division of Human Mechanical Systems and Design,
Graduate School of Engineering, Hokkaido University
N13 W8, Kita-ku, Sapporo, Hokkaido 060-8628, Japan
***Division of Human Mechanical Systems and Design, Faculty of Engineering, Hokkaido University
N13 W8, Kita-ku, Sapporo, Hokkaido 060-8628, Japan
E-mail:tadano@eng.hokudai.ac.jp

Abstract

The presence of residual stresses in bone tissue has been noted, and the authors have reported that there are residual stresses in bone tissue. The tensile residual stresses in the bone axial direction on the cortical surface of the bovine femoral diaphyses were measured by X-ray diffraction method with characteristic Mo-Kα X-rays. However, then the residual stresses inside the cortical bone could not be accurately determined. The study here used synchrotron white X-rays obtained from the BL28B2 beam line at SPring-8 and was able to measure the residual stresses in the bovine femoral diaphysis in depth. The measurement positions in the diaphysis specimen were at 1 mm intervals from the outer surface to the inner surface of the specimen in four parts of the diaphysis: anterior, posterior, lateral, and medial. The results showed that the residual stresses in the bone axial direction at the outer cortical surface were tensile and the stresses in the inner positions of the cortical bone were compressive. In the anterior part, the residual stress at the surface was 24.7 MPa. From 2 mm to 10 mm depths inside the diaphysis, compressive residual stresses were measured and the average of these stresses was -9.0 MPa.

Key words: Cortical Bone, Residual Stress, Synchrotron, X-ray Diffraction, Hydroxyapatite

1. Introduction

Cortical bone has a hierarchical and composite structure composed of hydroxyapatite (HAp) and collagen matrix. The HAp has a hexagonal crystal structure, and X-ray diffraction can be used to measure the interplanar spacings of HAp crystals in cortical bone [(1)-(4)]. When bone tissue deforms, the displacement of the lattice planes of the HAp crystals also changes [(1)], and the HAp strain can then be calculated by the deformation of the interplanar spacing from a reference stage [(2)(3)].

Living tissue such as blood vessels is subject to residual stress [(5)], and the presence of residual stress in bone tissue has also been noted [(6)]. The authors have proposed the $\sin^2\psi$ method of X-ray diffraction as a method to measure the residual stress in bone tissue [(7)]. In previous studies, the residual stresses at the outer cortical surface of the diaphysis of bovine femurs and rabbit limb bones were measured with characteristic Mo-Kα X-rays, and it was confirmed that there are tensile residual stresses in the bone axial direction [(7)(8)]. However, the residual stress inside the cortical bone would not be measured by this previous method.

*Received 12 Jan., 2011 (No. 11-0025)
[DOI: 10.1299/jbse.6.114]

The X-rays generated by an X-ray tube in the previous study can only penetrate about 100 μm into the specimen and the method is only effective to measure the outermost region of the bone. Synchrotron white X-rays form a highly collimated high-intensity X-ray beam that can pass through thick bone specimens like the femoral diaphysis. Some strain measurements of HAp crystals and collagen fibrils in bone tissue have been conducted with high-energy X-rays generated by a synchrotron radiation source [9]-[11].

The aim of this study is to measure the residual stress inside diaphysis specimens using synchrotron white X-rays. In the experiments here, a bovine femoral diaphysis was used and the distribution of residual stress from the outer surface to the inner region of cortical bone was measured.

2. Synchrotron Measurement Method

As suggested in Fig. 1, the interplanar spacing d of HAp crystals is uniform at the non-strained state, and the interplanar spacing d varies with the direction under tensile loading. The angle of inclination ψ is defined as the angle between the radial direction of the diaphysis specimen and the diffracted lattice plane. When the cortical bone is stretched in the bone axial direction, the interplanar spacing in the lattice planes for the $\psi = 90°$ direction is larger than that for the $\psi = 0°$ direction. The relation between d and ψ is affected by the amount of the stress and the tissue stress can be estimated from the d–ψ relation.

Fig. 2 shows the coordinate system employed here at each measurement position in the cortical bone. The x, y, and z-axes correspond to the bone axial, circumferential, and radial directions, and these axes are defined as the principal axes. Further, the study assumed that the diaphysis in the radial direction was not subject to residual stress.

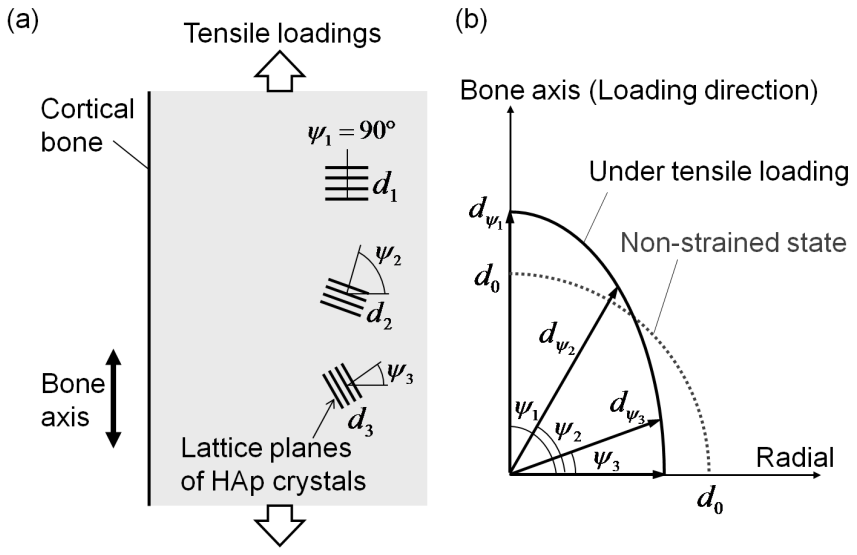

Fig. 1 Relationship between tissue stress σ^B and interplanar spacing d of HAp crystals. (a) Changes in the interplanar spacings d of HAp crystals oriented in different directions in the cortical bone under tensile loading. (b) Vector diagram of the interplanar spacing d of HAp crystals. The interplanar spacing of lattice planes oriented in the loading direction is the largest and that oriented normal to the loading direction is the smallest. The difference depends on the magnitude of the stress σ^B.

The relationship between wavelength λ and the energy W of X-rays is expressed as in Eq. (1), where h is Planck's constant and c is the speed of light.

$$\lambda = \frac{hc}{W} \tag{1}$$

Using Bragg's law, the fundamental equation for X-ray diffraction, the relationship between the interplanar spacing d of HAp crystals and the X-ray energy W is expressed as in Eq. (2)

$$d = \frac{hc}{2W\sin\theta}, \tag{2}$$

where θ is the Bragg angle and fixed during the measurements. The interplanar spacing d can be measured from the energy of the diffracted X-rays. The strain in the HAp lattice plane ε^H is defined as in Eq. (3), where d_0 is the interplanar spacing of the non-strained state.

$$\varepsilon^H = \frac{d - d_0}{d_0} \tag{3}$$

In this study, the relation between bone tissue stress σ^B and HAp strain ε^H in the cortical bone is assumed to be described by Eq. (4).

$$\begin{pmatrix} \varepsilon_x^H \\ \varepsilon_y^H \\ \varepsilon_z^H \end{pmatrix} = \begin{bmatrix} \frac{1}{E^*} & -\frac{\nu^*}{E^*} & -\frac{\nu^*}{E^*} \\ -\frac{\nu^*}{E^*} & \frac{1}{E^*} & -\frac{\nu^*}{E^*} \\ -\frac{\nu^*}{E^*} & -\frac{\nu^*}{E^*} & \frac{1}{E^*} \end{bmatrix} \begin{pmatrix} \sigma_x^B \\ \sigma_y^B \\ \sigma_z^B \end{pmatrix} \tag{4}$$

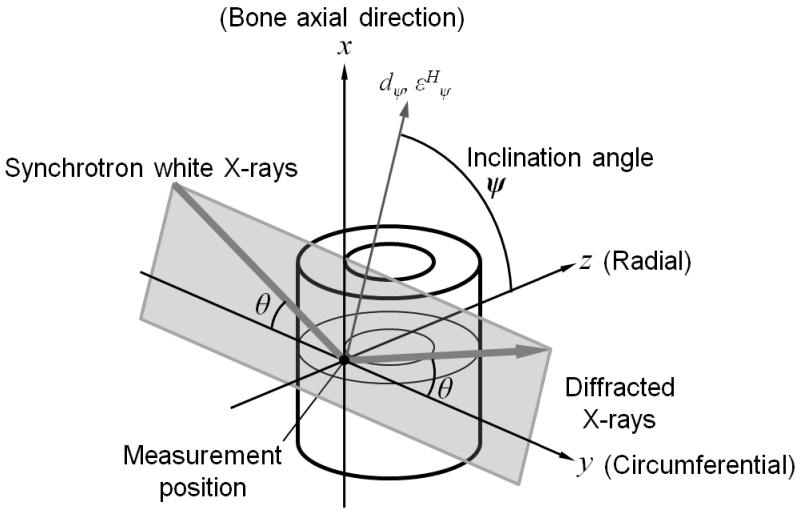

Fig. 2 Coordinate system at a measurement position in the cortical bone.

It is possible to measure the HAp strain ε^H_ψ for an angle of inclination ψ as shown in Fig. 2, and ε^H_ψ is described with ε^H_x and ε^H_z as in Eq. (5).

$$\varepsilon^H_\psi = \varepsilon^H_x \sin^2\psi + \varepsilon^H_z (1 - \sin^2\psi) \tag{5}$$

Here, the study assumed $\sigma^B_z = 0$. Equation (5) can be expressed as Eq. (6) using Eq. (4).

$$\varepsilon^H_\psi = \frac{1+\nu^*}{E^*}\sigma^B_x \sin^2\psi - \frac{\nu^*}{E^*}(\sigma^B_x + \sigma^B_y) \tag{6}$$

By partial differentiation of Eq. (6) with respect to ($\sin^2\psi$), the following expression is derived.

$$\frac{E^*}{1+\nu^*}\frac{\partial\varepsilon^H_\psi}{\partial(\sin^2\psi)} = \sigma^B_x \tag{7}$$

Therefore, σ^B_x can be described with the interplanar spacing d_ψ and ψ as in Eq. (8)

$$\sigma^B_x = \frac{E^*}{d_0(1+\nu^*)}\frac{\partial d_\psi}{\partial(\sin^2\psi)} \equiv K_d \frac{\partial d_\psi}{\partial(\sin^2\psi)}, \tag{8}$$

where K_d is the stress constant. This allows the residual stress in the bone axial direction in cortical bone to be estimated from Eq. (8).

In the current study, the interplanar spacings of the (002) plane of HAp crystal were measured to calculate the residual stress. In the previous study, the stress constant of the (211) plane was measured with characteristic Mo-Kα X-rays (λ = 0.07107 nm) as $K_{2\theta(211)}$ = -660 MPa/deg [7]. In the current study, the stress constant K_d (MPa/nm) of the (002) plane was calculated from that of the (211) plane considering the ratio of lattice strains of the (211) plane to the (002) plane during certain loading, as described in Eq. (9).

$$K_d = -\frac{360\tan\theta_{0(211)}}{\pi d_{0(002)}} C \cdot K_{2\theta(211)} \tag{9}$$

In Eq. (9), $d_{0(002)}$ is the interplanar spacing of the (002) plane in the non-strained state and $\theta_{0(211)}$ is the Bragg angle of the (211) plane with characteristic Mo-Kα X-rays in the non-strained state. Further, C indicates the ratio of lattice strains of the (211) plane to the (002) plane during certain loading, and was measured as C = 0.75 [1] with tensile tests in the previous study.

3. Experiments

A fresh femur was obtained from a 26-month-old bovine and frozen at -35 °C until further preparation. The study used the mid-diaphysis part of the cortical bone. The diaphysis specimen was 60 mm long in the bone axial direction and cut using a slow speed diamond wheel saw (SBT650: South Bay Technology Inc., USA), and the measurement position was the center of the femur and the diaphysis specimen respectively (Fig. 3). The bone marrow and the soft tissue around the surfaces were removed and the specimen was air dried at room temperature. To fix the specimen on the measurement instruments for the X-ray diffraction, one end of the specimen was bonded to an acrylic plate with epoxy resin.

The measurement points in the diaphysis specimen were sited at 1 mm intervals from the outer surface to the inner region of the specimen at four parts of the diaphysis: anterior (A), posterior (P), lateral (L), and medial (M), as shown in Fig. 4.

The synchrotron white X-ray diffraction was performed at the BL28B2 beam line of SPring-8, Japan Synchrotron Radiation Research Institute (JASRI). As shown in Fig. 5, the specimen was irradiated with the X-ray beam (Incident angle $\theta = 2.5°$), and the beam, with intensity optimized with an aluminum absorber, was collimated with a slit (Slit 1: 200 μm high, 200 μm wide). The diffraction angle 2θ was set to 5° during the measurements. Scattered X-rays were eliminated from the diffracted X-rays by two slits (Slits 2 and 3: 200 μm high, 150 μm wide). The diffracted X-rays were detected by a solid state detector (SSD) and the pulse height distribution of the X-rays was analyzed by a multichannel analyzer (MCA) (4096 channels). Fluorescent X-rays of Pb-Kα1 and Sn-Kα1 were measured to calibrate the MCA.

The interplanar spacing d_ψ was measured at the following ψ conditions: 90.0°, 71.6°, 63.4°, and 56.8° by tilting the specimen set on a swivel stage, and $\partial d_\psi / \partial(\sin^2\psi)$ in Eq. (8)

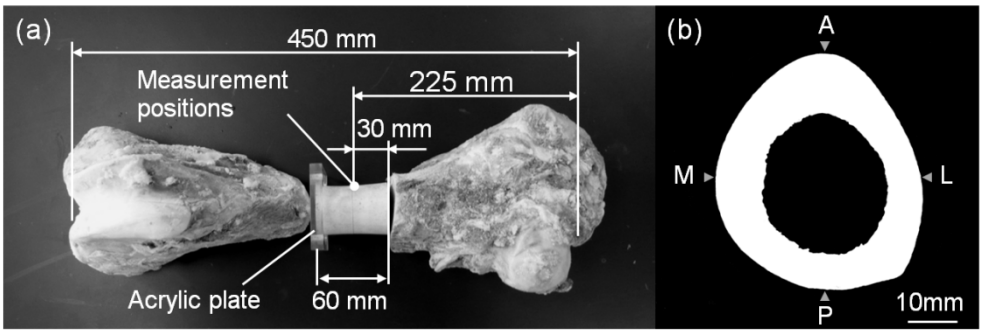

Fig. 3 Diaphysis specimen. (a) The specimen was taken from the middle diaphysis of a bovine femur. The measurement position was the center of the femur and the diaphysis specimen, respectively. To fix the specimen on the measurement instruments, one end of the specimen was bonded to an acrylic plate with epoxy resin. (b) The cross-section shape at the measurement positions of the specimen. The image was observed cutting the specimen after the X-ray measurements. Triangle marks in the image indicate the measurement parts: anterior (A), posterior (P), lateral (L), and medial (M).

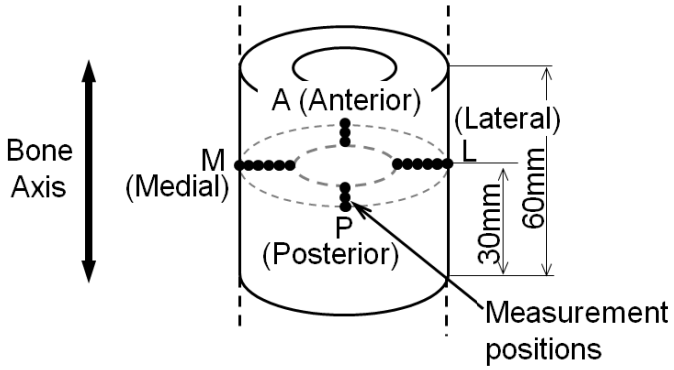

Fig. 4 Measurement positions in the diaphysis specimen. The positions are sited at 1 mm intervals from the outer surface toward the inside of the specimen at four parts: anterior (A), posterior (P), lateral (L), and medial (M).

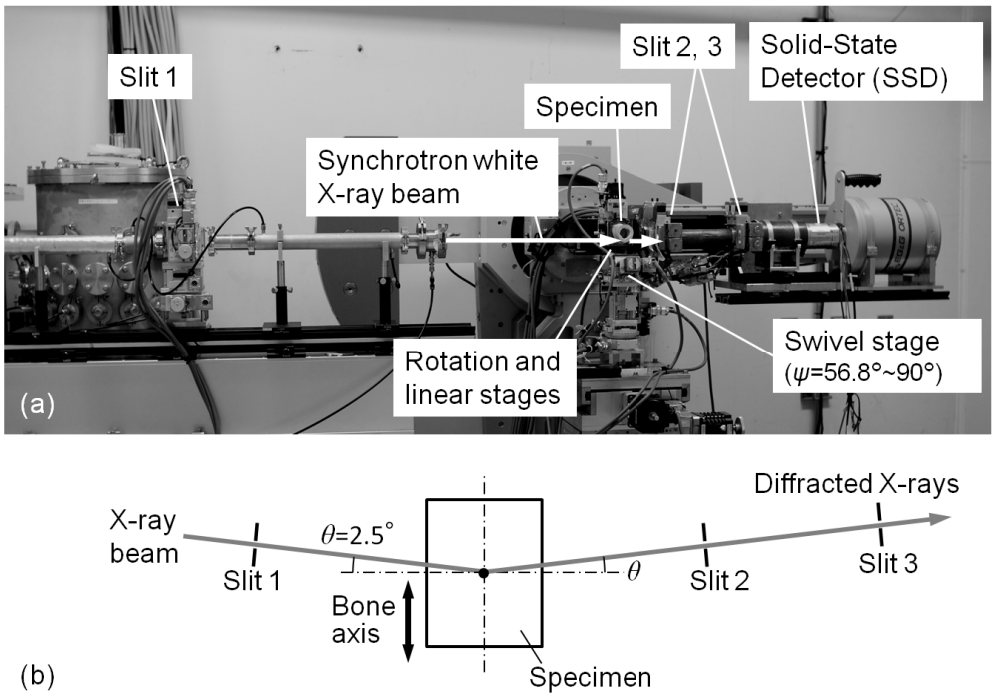

Fig. 5 (a) Measurement setup for X-ray diffraction at the BL28B2 in SPring-8. The specimen was fixed on a swivel stage to enable changes in the ψ angle (90.0°, 71.6°, 63.4°, and 56.8°). The synchrotron white X-ray beam was collimated with a slit (Slit 1: 200 μm high, 200 μm wide). The diffracted X-rays were detected by a solid state detector (SSD). Scattered X-rays were eliminated from the diffracted X-rays with two slits (Slits 2 and 3: 200 μm high, 150 μm wide). (b) Top view of the setup at ψ = 90°. The specimen was irradiated with the X-ray beam (Incident angle θ = 2.5°), and the diffraction angle 2θ was fixed at 5°.

was calculated by the linear least-squares method. The exposure time was 120 seconds at each ψ condition. To calculate the interplanar spacing d_ψ, the peak of the (002) plane in the spectrum was used.

4. Results

Figure 6 shows the X-ray diffraction profile of the diaphysis specimen. The horizontal axis indicates the energy of diffracted X-rays. The value of the energy was calculated from the channel number analyzed by the MCA with the fluorescent X-rays of Pb and Sn. The peak of the (002) plane in the HAp crystals was sharp with a distinct highest intensity, and the peak position was determined as the midpoint of the full width at two-thirds maximum intensity of the profile (FWTTM method) using the energy range between 39.8 and 43.1 keV.

Figure 7 shows the relationship between $d_{(002)}$ and $\sin^2\psi$ at the outer surface (depth = 0 mm) of the anterior part. The coefficient of correlation R^2 was 0.97 in this relation showing that d_ψ and $\sin^2\psi$ are strongly correlated. The values of $\partial d_\psi/\partial(\sin^2\psi)$ at each position were calculated from the relations by the linear least-squares method. The measurements at other positions also show strong correlations, except when $\partial d_\psi/\partial(\sin^2\psi)$ was close to zero. The stress constant K_d could be calculated as K_d = 21000 MPa/nm from the $K_{2\theta(211)}$ and C established in the previous studies with Eq. (9). Then, the residual stresses can be calculated from the K_d and $\partial d_\psi/\partial(\sin^2\psi)$.

Figure 8 shows the radial distribution of the residual stress in the bone axial direction from the outer surface to the inner region of the diaphysis specimen at the four parts: anterior, posterior, lateral, and medial. The values of residual stresses were calculated from one measurement at each position. The horizontal axis indicates the depth of the measurement positions from the outer surface of the specimen at each part. The thicknesses of the specimen at anterior, posterior, lateral, and medial parts were 12.0 mm, 7.3 mm, 7.1 mm, and 10.0 mm, respectively (Fig. 3(b)). The deepest positions indicated in Fig. 8 do not correspond to the inner surface of the diaphysis specimen, because the intensity of the diffracted X-rays around the inner surface region was too low to calculate d_{ψ}. Since the X-ray pathway at anterior part was shorter than that at the other parts, residual stress in the deepest region could be measured at anterior part.

At the outer surface, there were tensile residual stresses at the four parts and that trend corresponded to those in the previous study of bovine femoral diaphyses [7]. In the anterior part, the residual stress at the surface was 24.7 MPa and that at 1 mm depth was 2.5 MPa. Inside the diaphysis, from 2 mm to 10 mm depths, there were compressive residual stresses. The average of these stresses in the inner region was -9.0 MPa, smaller than the stress at the surface. In the posterior and medial parts, there were also tensile residual stresses at the surface with values of 9.2 MPa and 8.2 MPa, respectively. The inner cortical bone here

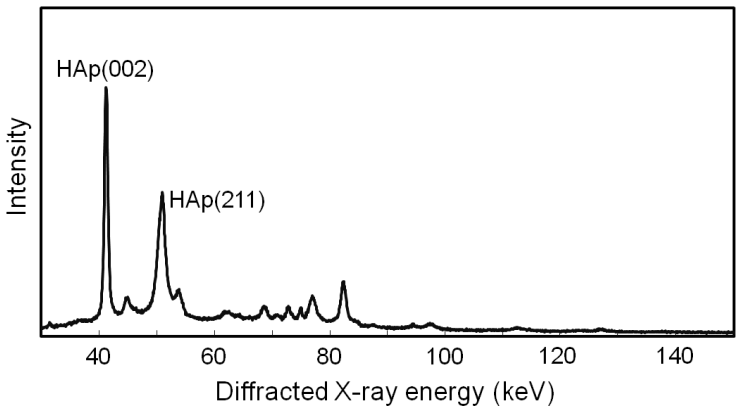

Fig. 6 Typical diffracted X-ray profile of the diaphysis specimen using the synchrotron white X-rays.

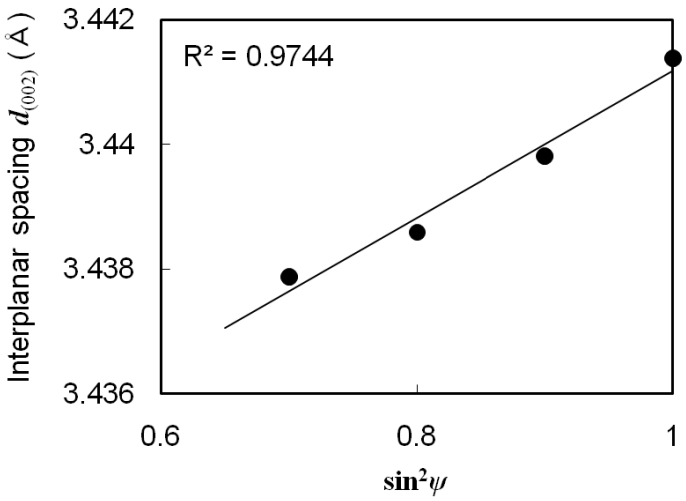

Fig. 7 Typical relationship between $d_{(002)}$ and $\sin^2\psi$ at the outer surface (depth = 0 mm), anterior part (A).

was subject to compressive residual stresses as in the anterior part. There was a highest compressive stress at 5 mm depth in the medial part. In the lateral part, there was tensile stress both at the surface and down to 4 mm depth, here the average stress was 4.2 MPa. The position at 5 mm depth in the lateral part was subjected to compressive stress like the other parts.

5. Discussion

In the study, the distribution of residual stress in the bone axial direction was mapped by measuring the residual stresses at 1 mm intervals from the outer surface to the inner region of the specimen at four parts. The measured residual stress at each position was the average in the measured volume as shown in Fig. 9. The volume was determined by the slit sizes, the position of the slits, and the diffraction angle. The volume was a parallelepiped and the maximum length was 5590 μm. The longitudinal direction of the volume was aligned along the circumferential direction of the diaphysis specimen.

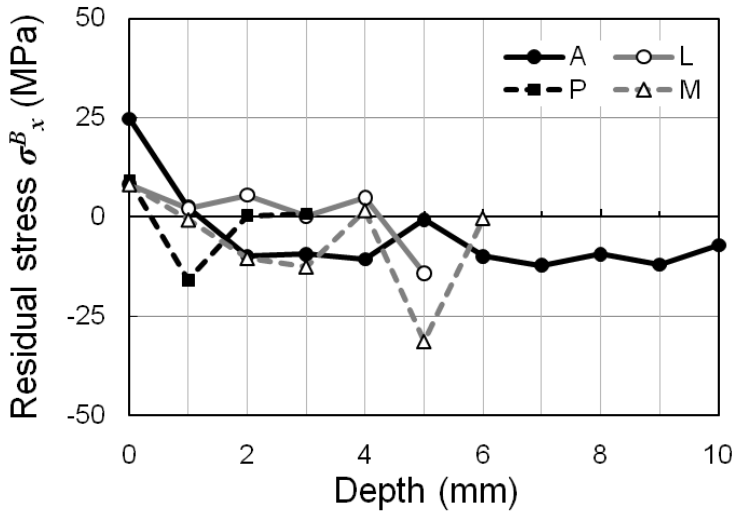

Fig. 8 Radial distribution of the residual stress in the bone axial direction from the outer surface to the inside of the diaphysis specimen at the four parts: anterior (A), posterior (P), lateral (L), and medial (M).

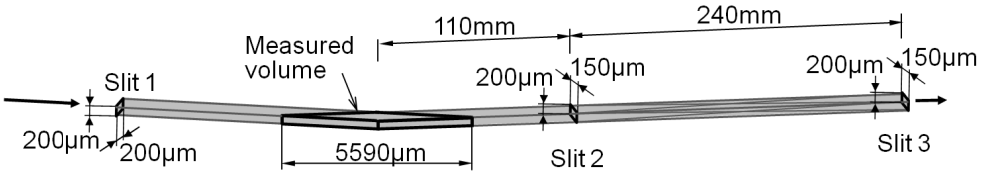

Fig. 9 Measured volume of X-ray diffraction in each position. The measured volume was decided by the slit sizes, the length between the slits, and the diffraction angle (2θ = 5°). The volume was a parallelepiped (approximately 200 × 290 × 5590 μm) and the longitudinal direction of the volume was aligned along the circumferential direction of the diaphysis specimen.

As shown in Fig. 8, the outer surface in the bovine femoral diaphysis were subjected to tensile residual stress and the inner region of the cortical bone was subjected to compressive stress. Further, the magnitude of the tensile residual stress at the surface was larger than that of the compressive stress in the inner region. The highest compressive stress was at 5 mm depth in the medial part. The stress value at this point may reflect deviations due to the lower intensity of the X-rays. It may also reflect differences of the microstructure between this and neighboring measurement positions.

The sum of the value of residual stresses from the outer surface to the inner region in depth was -54.0 MPa at anterior, -5.6 MPa at posterior, 6.8 MPa at lateral, and -45.5 MPa at medial part. At posterior and lateral parts, residual stress may equilibrate the stresses of the outer surface and the inner region in depth; however, the quantitative equilibrium of residual stresses could not be determined because of a deviation in one measurement in this study.

Previously the focus was on residual stresses at the cortical surface of the limb bones [7][8]. The diaphysis surface would be subject to high mechanical loadings in vivo due to bending and torsional loadings. In the current study, there were gradients in the residual stress in the surface layers. The surface layer will need to be the focus of further study to understand the mechanism of generation of residual stress in bone tissue.

The study assumed that the diaphysis specimen in the radial direction was not subject to residual stresses. It is well known that bone is usually replaced by new bone tissue with constructing osteon structures [5][12]. Since the new tissue is constructed under in vivo loading as the non-deformed state, an indeterminate structure may be generated by differences in the deformation of the old and new phases. The residual stress in the bone tissue may be generated by nonuniform structures related to osteons in the bone tissue and may be related to the in vivo mechanical loading. Therefore, it would appear that the radial direction may not be subject to residual stresses, since the diaphysis specimen in the radial direction is subject to only small applied stresses in vivo. Figure 10 shows the radial distribution of the interplanar spacing $d_{(002)}$ of the (002) lattice plane in the bone axial direction. The interplanar spacings were measured at $\psi = 90°$. Focusing on the distribution of the anterior part, the interplanar spacing of the HAp crystals at the surface was larger

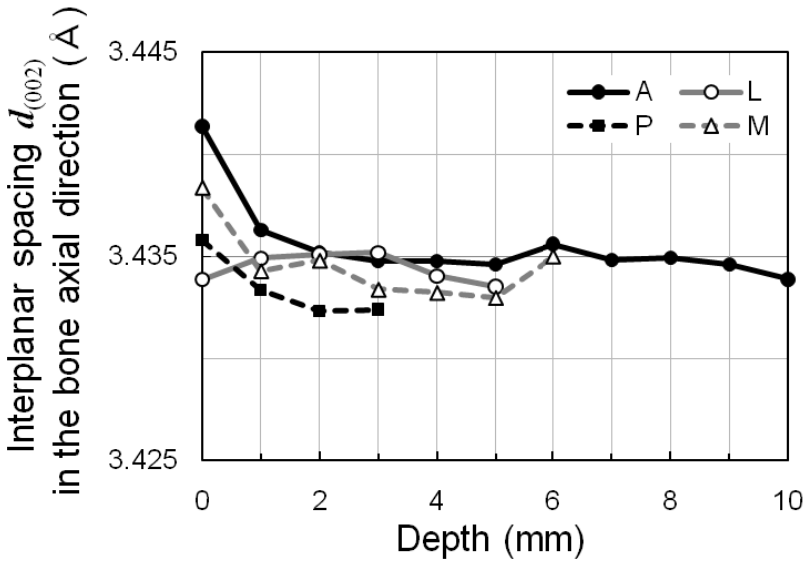

Fig. 10 Radial distribution of the interplanar spacing $d_{(002)}$ of the (002) lattice plane in the bone axial direction ($\psi = 90°$) from the outer surface to the inside of the diaphysis specimen at the four parts: anterior (A), posterior (P), lateral (L), and medial (M).

than that in the inner positions. The distribution of interplanar spacings closely corresponds to the distribution of residual stresses. This suggests that the deviatoric HAp strain in the bone axial direction will correspond to the residual stress in the bone axial direction. This would suggest the conclusion that even when the study includes the radial component in the measured residual stress, this component may have little effect on the measured values.

6. Conclusion

In this study, the distribution of residual stresses in the bovine femoral diaphysis can be measured using synchrotron white X-ray diffraction. The residual stresses in the bone axial direction at the outer cortical surface were tensile and the stresses in the inner region of the cortical bone were compressive. In the anterior part, the residual stress at the surface was 24.7 MPa. From 2 mm to 10 mm depths inside the diaphysis, compressive residual stresses were measured and the average of these stresses was -9.0 MPa.

Acknowledgment

This work was supported by Grant-in-Aid for Scientific Research (A) (No. 19200035) and Grant-in-Aid for JSPS Fellows (No. 09J00736). The synchrotron radiation experiments were performed at the BL28B2 of SPring-8 with the approval of the Japan Synchrotron Radiation Research Institute (JASRI) (Proposal No. 2010A1592) and supported by Dr. Kentaro KAJIWARA (JASRI).

References

(1) Fujisaki, K., and Tadano, S., "Relationship between Bone Tissue Strain and Lattice Strain of HAp Crystals in Bovine Cortical Bone under Tensile Loading", *Journal of Biomechanics*, Vol. 40, No. 8 (2007), pp. 1832-1838.

(2) Fujisaki, K., Tadano, S., and Sasaki, N., "A Method on Strain Measurement of HAp in Cortical Bone from Diffusive Profile of X-ray Diffraction", *Journal of Biomechanics*, Vol. 39, No. 3 (2006), pp. 579-586.

(3) Tadano, S., Giri, B., Sato, T., Fujisaki, K., and Todoh, M., "Estimating Nanoscale Deformation in Bone by X-ray Diffraction Imaging Method", *Journal of Biomechanics*, Vol. 41, No. 5 (2008), pp. 945-952.

(4) Giri, B., Tadano, S., Fujisaki, K., and Sasaki, N., "Deformation of Mineral Crystals in Cortical Bone Depending on Structural Anisotropy", *Bone*, Vol. 44, No. 6 (2009), pp. 1111-1120.

(5) Fung, Y.C., *Biomechanics: Motion, Flow, Stress, and Growth*, (1990), p. 388-393, 500-503, Springer.

(6) Tadano, S., and Okoshi, T., "Residual stress in bone structure and tissue of rabbit's tibiofibula", *Bio-Medical Materials and Engineering*, Vol. 16 (2006), pp.11–21.

(7) Yamada, S., and Tadano, S., "Residual Stress Around the Cortical Surface in Bovine Femoral Diaphysis", *Transactions of the ASME, Journal of Biomechanical Engineering*, Vol. 132, No. 4 (2010), pp. 0445031-0445034.

(8) Yamada, S., Tadano, S., Todoh, M., and Fujisaki, K., "Residual Stresses at the Cortical Bone of the Rabbit Extremities", *IFMBE Proceedings - WCB2010*, Vol. 31 (2010), pp. 780-783.

(9) Gupta, H. S., Seto, J., Wagermaier, W., Zaslansky, P., Boesecke, P., and Fratzl, P., "Cooperative Deformation of Mineral and Collagen in Bone at the Nanoscale", *PNAS*, Vo. 103, No. 47 (2006), pp. 17741-17746.

(10) Almer, J. D., and Stock, S. R., "Internal Strains and Stresses Measured in Cortical Bone via High-energy X-ray Diffraction", *Journal of Structural Biology*, Vol. 152, No. 1 (2005), pp. 14-27.
(11) Almer, J. D., and Stock, S. R., "Micromechanical Response of Mineral and Collagen Phases in Bone", *Journal of Structural Biology*, Vol. 157, No. 2 (2007), pp. 365-370.
(12) Currey, J.D., *Bones: structure and mechanics*, (2002), p. 14-21, Princeton University Press.